Posted on 21 Nov 2022 — The copyright holder is the author/funder. All rights reserved. No reuse without permission. — https://doi.org/10.1002/essoar.10505309.1 — This a preprint and has not been peer reviewed. Data may be preliminary.

Impact of recent warming in East Asian marginal seas on the heavy rainfall event occurred in Kyushu Island, Japan in July 2017

Atsuyoshi Manda[1]

[1]Mie University

November 21, 2022

Abstract

There are growing evidences that the warming marginal seas impact the torrential rainfall events in many parts of the world. The sea surface temperature (SST) in the East Asian marginal seas (EAMS) exhibits rapid rise during the last decades compared to the global mean, but its impact is still a matter of debate. Here we assess the impact of the recent warming trend of the EAMSs on the torrential rainfall event that caused devastating flooding and landslides in Kyushu Island located in the western part of Japan in July 2017, using a high-resolution cloud permitting model. The warming trend of EAMS with atmospheric warming since 1980s increases the simulated 12-hr precipitation to 6.8%, corresponding to approximately 10% increase per 1 K of SST rise, consistent with the previous data analysis study. Slight increase in heat and moisture supplies due to the warming EAMS has impacted a conditionally unstable condition of air masses flowing into an area of the precipitation, leading to more vigorous convective systems. Moisture budget analysis indicates that the changes in the amount of precipitation is not responsible for the availability of precipitable water but the intensification of the convective system. Since the change in precipitation amount exhibits high sensitivity to the SST trends, use of multiple SST datasets is desirable to provide a more reliable estimate and its uncertainty.

Impact of recent warming in East Asian marginal seas on the heavy rainfall event occurred in Kyushu Island, Japan in July 2017

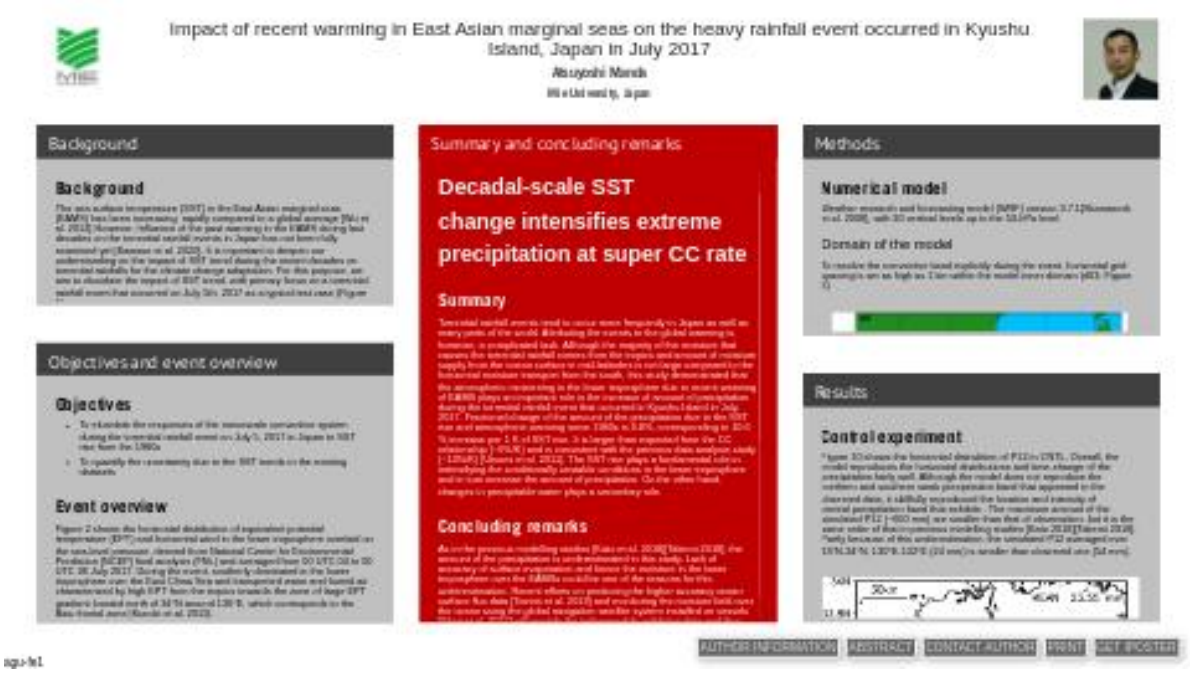

Atsuyoshi Manda

Mie University, Japan

PRESENTED AT:

BACKGROUND

Background

The sea surface temperature (SST) in the East Asian marginal seas (EAMS) has been increasing rapidly compared to a global average [Wu et al. 2012].However, Influence of the past warming in the EAMS during the last decades on the torrential rainfall events in Japan has not been fully examined yet [Kawase et al. 2020]. It is important to deepen our understanding on the impact of SST trend during the recent decades on torrential rainfalls for the climate change adaptation. For this purpose, we aim to elucidate the impact of SST trend, with primary focus on a torrential rainfall event that occurred on July 5th, 2017 as a typical test case (Figure 1).

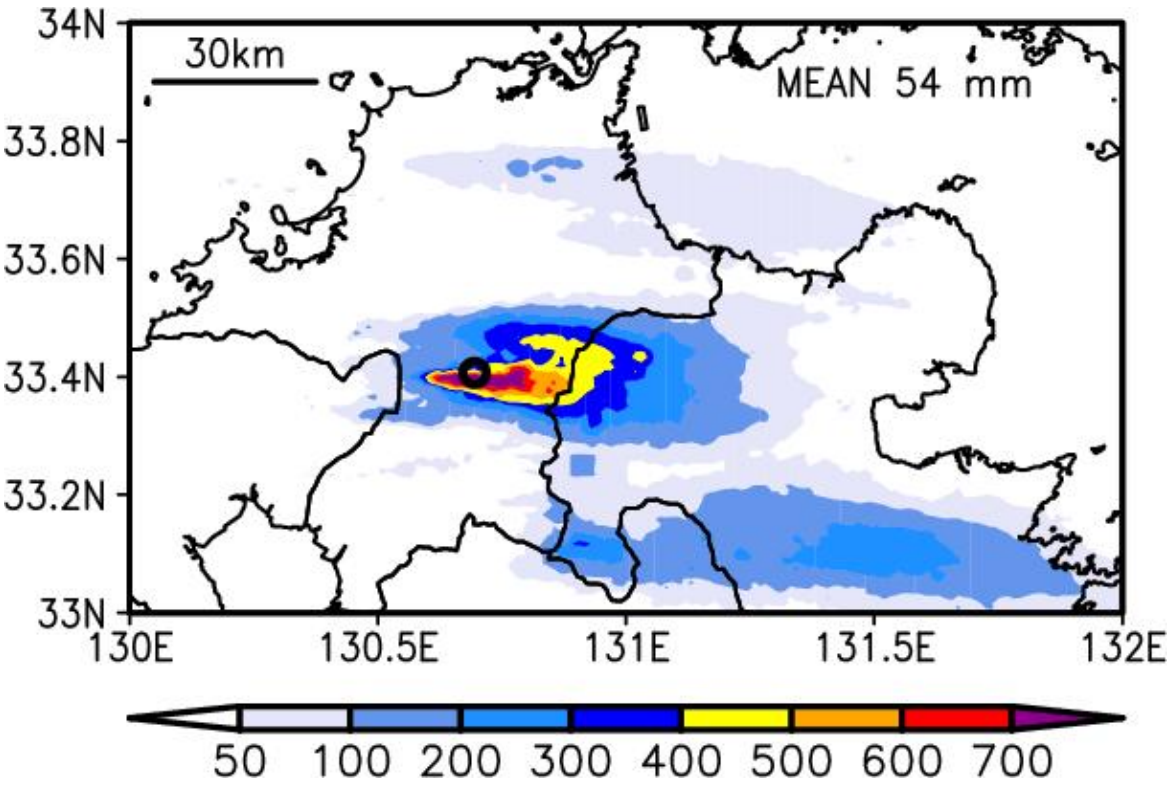

Figure 1 Horizontal distribution of 12-hr accumulated precipitation (mm) from 01 to 13 UTC 05 July 2017 using a gridded precipitation analysis produced by Japan Meteorological Agency.

In that event, line-shaped quasi-stationary convective systems, which are one of the major precipitation systems that cause severe flooding and landslides in Japan [Unuma and Takemi 2016], occurred and caused a rainfall with 24-hour totals exceeding 700 mm, with records set at a weather station in the northern Kyushu Island [Kato et al. 2018; Takemi 2018]. A severe flooding due to this event caused more than 40 casualties and more than 1500 flooded houses.Despite its significance and severity, the impact of the warming of EAMS on the event has not been examined yet.

Recent study shows that the uncertainty in the SST datasets affect the intensity and locations of simulated precipitation [Iizuka and Nakamura 2019], suggesting that single simulation using only one SST dataset leads to inaccurate estimation of precipitation. Thus, use of multiple SST datasets should be desirable in order to assess the impact of SST on the torrential rainfall events.

OBJECTIVES AND EVENT OVERVIEW

Objectives

- To elucidate the responses of the mesoscale convective system during the torrential rainfall event on July 5, 2017 in Japan to SST rise from the 1980s
- To quantify the uncertainty due to the SST trends in the existing datasets

Event overview

Figure 2 shows the horizontal distribution of equivalent potential temperature (EPT) and horizontal wind in the lower troposphere overlaid on the sea-level pressure, derived from National Center for Environmental Prediction (NCEP) final analysis (FNL) and averaged from 00 UTC 04 to 00 UTC 06 July 2017. During the event, southerly dominated in the lower troposphere over the East China Sea and transported warm and humid air characterized by high EPT from the tropics towards the zone of large EPT gradient located north of 34°N around 130°E, which corresponds to the Baiu frontal zone [Kunoki et al. 2015].

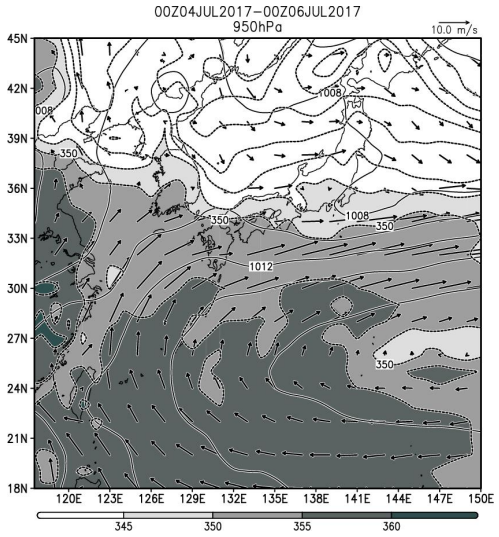

Figure 2. Horizontal distribution of the equivalent potential temperature in K (shade) and horizontal wind (vectors) at 950 hPa level overlaid on sea level pressure in hPa (solid contour), averaged from 00 UTC 04 to 00 UTC 06 July 2017.

The water vapor mixing ratio and EPT exceeded 18 g/kg and 360 K, respectively in the lowest part of the troposphere (Figure 3). This warm and humid air set up the convectively unstable condition south of the Baiu frontal zone in the lower troposphere.

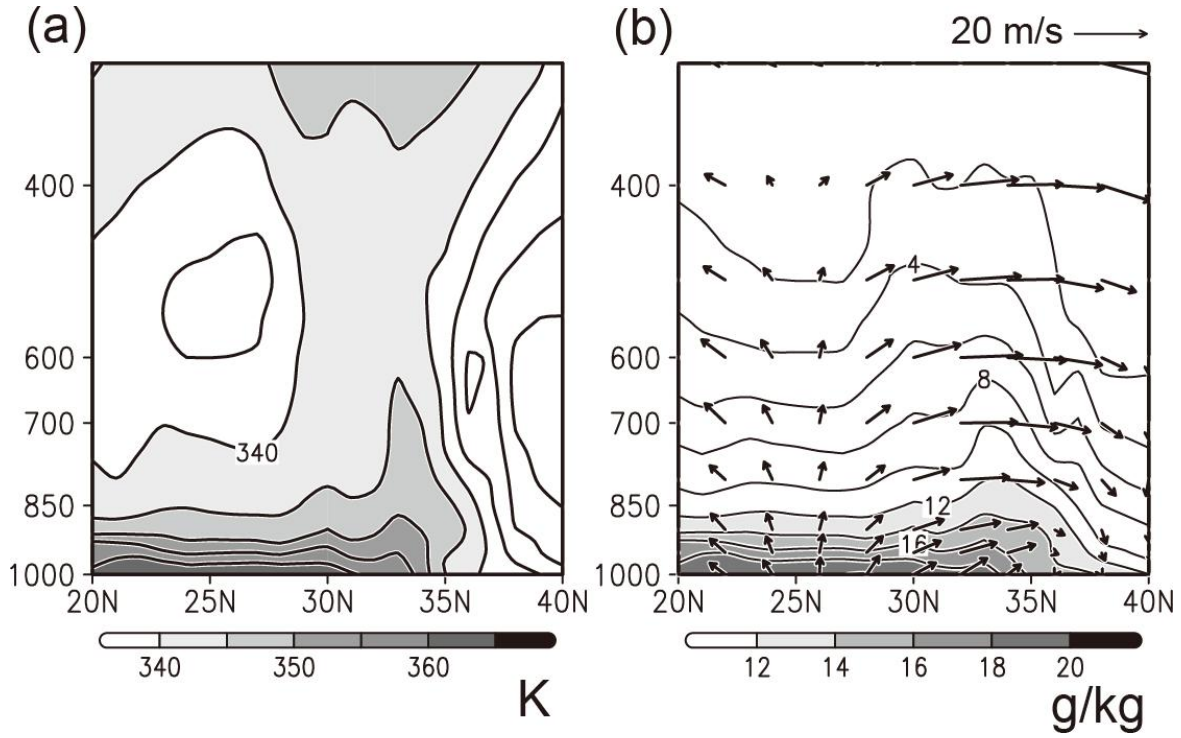

Figure 3. Latitude-pressure diagrams of (a) equivalent potential temperature in K and (b) water vapor mixing ratio in g/kg (contour) and horizontal wind (vector) along 130°E, averaged from 00 UTC 04 to 00 UTC 05 July 2017. Upward (rightward) vector indicates southerlies (westerlies).

It also contributes to high convective available potential energy (CAPE) and low convective inhibition (CIN) in the lower troposphere (Figure 4). Both lifting condensation level (LCL) and level of free convection (LFC) are low around Kyushu Island (~32°N); LCL is well below 900 hPa level and LFC is at approximately 850 hPa. They all provide an environment for a high chance of deep moist convection and a typical condition for torrential rainfall events in the Kyushu Island during warm season [Kato et al. 2003].

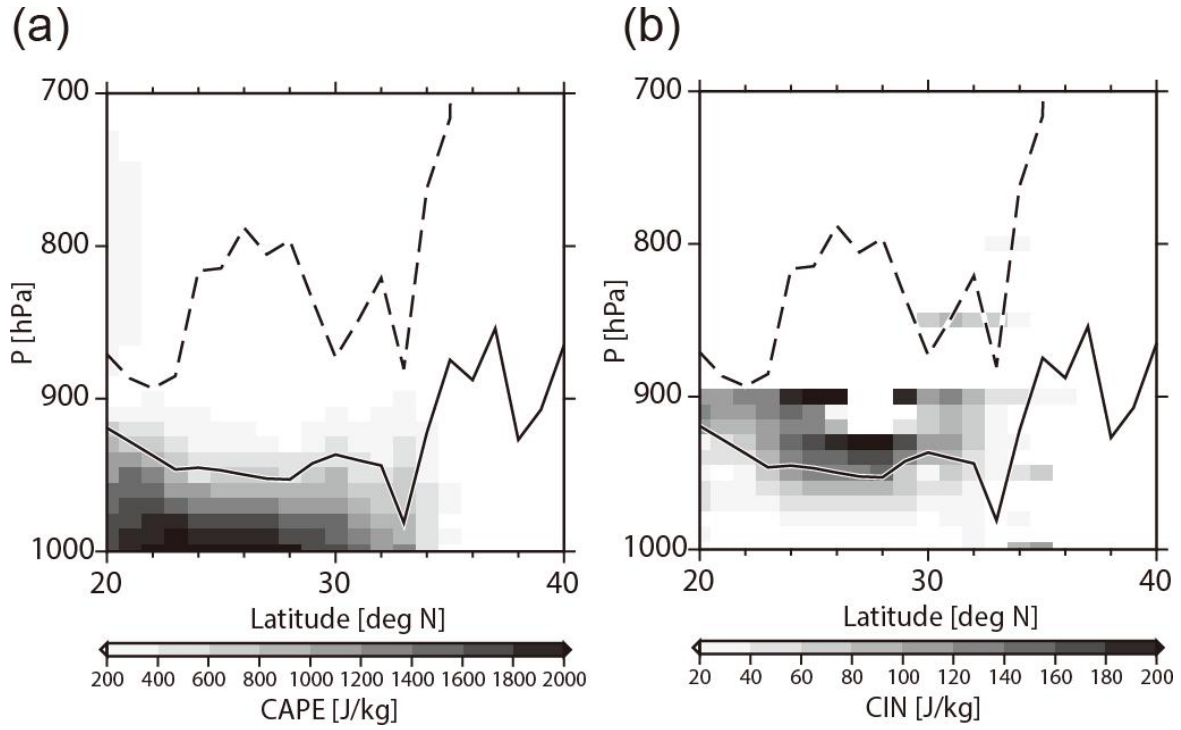

Figure 4. Latitude-pressure diagrams of (a) convective available potential energy and (b) convective inhibition along 130°E. Solid and dashed lines indicate lifting condensation level and level of free convection, respectively.

Figure 5 shows time-latitude diagram of hourly precipitation. It shows three distinct zonally oriented precipitation bands occurred during the period from 01 to 13 UTC July 2017. The highest accumulated precipitation was observed in the middle precipitation band among the three (Figures 1 and 5). In addition, there were other weak and moderate precipitation bands north and south of the most intense precipitation band, respectively.They indicate that these precipitation bands were almost stagnant in the meridional direction. This stagnancy contributes to the observed high accumulated precipitation in the northern part of Kyushu Island.

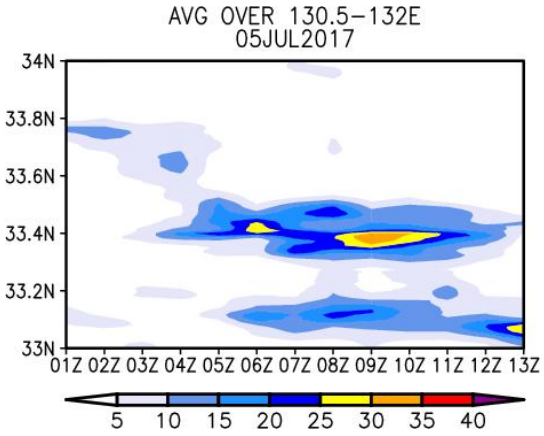

Figure 5 Time-latitude diagram of the hourly precipitation averaged over 130.5°E-132.0°E.

SUMMARY AND CONCLUDING REMARKS

Decadal-scale SST change intensifies extreme precipitation at super CC rate

Summary

Torrential rainfall events tend to occur more frequently in Japan as well as many parts of the world. Attributing the events to the global warming is, however, a complicated task. Although the majority of the moisture that causes the torrential rainfall comes from the tropics and amount of moisture supply from the ocean surface in mid-latitudes is not large compared to the horizontal moisture transport from the south, this study demonstrated that the atmospheric moistening in the lower troposphere due to recent warming of East Asian marginal seas plays an important role in the increase of amount of precipitation during the torrential rainfall event that occurred in Kyushu Island in July, 2017. Fractional change of the amount of the precipitation due to the SST rise and atmospheric warming since 1980s is 6.8%, corresponding to 10.6 % increase per 1 K of sea surface temprature (SST) rise. It is larger than expected from the Clausius-Clapeyron relationship (~6%/K at 25 degree Celsius) and is consistent with the previous data analysis study (~10%/K) [Utsumi et al. 2011]. The SST rise plays a fundamental role in intensifying the conditionally unstable conditions in the lower troposphere and in turn increase the amount of precipitation. On the other hand, changes in precipitable water plays a secondary role.

Concluding remarks

As in the previous modelling studies [Kato et al. 2018][Takemi 2018], the amount of the precipitation is underestimated in this study. Lack of accuracy of surface evaporation and hence the moisture in the lower troposphere over the EAMSs could be one of the reasons for this underestimation. Recent efforts on producing the higher accuracy ocean surface flux data [Tomita et al. 2019] and monitoring the moisture field over the ocean using the global navigation satellite system installed on vessels [Shoji et al. 2017] will provide the indispensable validation data and thus significantly contribute to the improvement of the numerical simulations. The deficiency of the numerical model itself could be another possible reason. The numerical models used in the previous and present studies employ different parameterizations, grid spacings, model domains, and initial and boundary conditions, but simulate the same order of accumulated rainfall. Although necessary, further refinement of the model is a complicated task. It is beyond the scope of this study, but it should be investigated in the future to provide the more reliable estimate of the precipitation.

In Japan, the torrential rainfall events have a broad spectrum with varieties of environmental synoptic conditions and precipitation systems. One of the examples showing such spectrum is the “heavy Rain Event of July 2018 in Japan” that caused devastating flooding and landslides in wide areas in the western part of Japan [Kawase et al. 2020]. Synoptic dynamical forcing plays a more important role in the event of 2018, compared to that of 2017 [Yokoyama et al. 2020]. Besides, majority of the convective clouds that contribute to a precipitation amount are less tall than that of 2017 event, suggesting responses of the precipitation systems to the SST change are different between these events. Comparative study is a fruitful way for deeper understanding of the impact of the warming EAMSs on the torrential rainfall events and contributes to more reliable future projections. In addition, long-term simulation (decades or so) is desirable to provide more reliable estimates of the impact of the long-term trend of SST on the precipitation extrema from the statistical viewpoint [Fujibe 2015].

METHODS

Numerical model

Weather research and forecasting model (WRF) version 3.7.1[Skamarock et al. 2008], with 30 vertical levels up to the 50-hPa level.

Domain of the model

To resolve the convective systems explicitly during the event, horizontal grid spacing is set as high as 1 km within the model inner domain (d03; Figure 6).

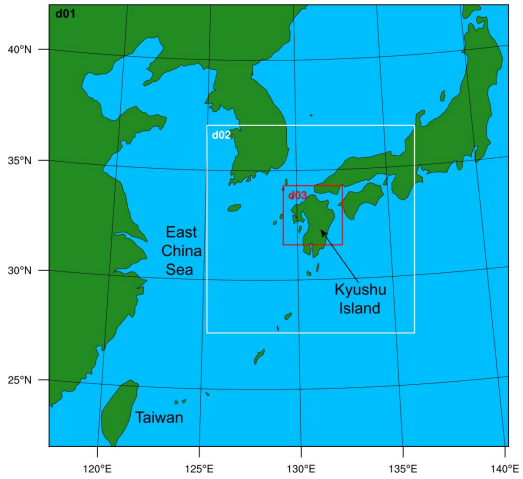

Figure 6 Map showing the outer domain of the numerical model used in this study. Inset squares indicate (white) intermediate and (red) inner domains.

Subgrid-scale parametalizations

- The new Kain-Fritsch convective parameterization scheme [Kain et al. 2004] (intermediate and outer domains)
- No such scheme was used for the inner domain to represent convective clouds
- Milbrandt-Yau 2-moment microphysics scheme [Milbrandt et al. 2005],
- Yonsei University planetary boundary layer scheme [Hong et al. 2006]
- Unified Noah land surface model [Tewari et al. 2004].
- Choice of these schemes are based on the prerimilary experiments using various microphysical and boundary layer schemes, namely, WRF Single-moment 3- and 6-class schemes, Thompson Scheme, Goddard Scheme, Morrison 2-moment Scheme, CAM V5.1 2-moment 5-class Scheme, Stony-Brook University Scheme, WRF Double Moment 5- and 6-class schemes, YSU, Mellor-Yamada-Janjic Scheme, Quasi-normal Scale Elimination Scheme, Mellor-Yamada-Nakanishi-Niino level 2.5 and 3 schemes, and the schemes described above.

Atmospheric Data

- NCEP final analysis
- NCEP reanalysis 1 [Kalnay et al. 1996] and 2 [Kanamitsu et al. 2002]
- ERA-Interim [Dee et al. 2011] and ERA5 [C3S 2017],
- JRA55 [Kobayashi et al. 2015]

Oceanic data

- Global High Resolution Sea Surface Temperature (GHRSST) Level 4 sea surface temperature analysis produced at the Naval Oceanographic Office (NAVO)
- COBE SST [Ishii et al. 2005]
- HadISST [Rayner et al. 2003]

- ERSST [Huang et al. 2017]
- MGDSST [Sakurai et al. 2005]
- OISST [Reynolds et al. 2007]

Experiment Description

Control experiment (CNTL)

Model integrations start from 1200 UTC 03 July, approximately 36 hours prior to the event. NAVO SST is used for the lower boundary condition over the ocean (Figure 7).

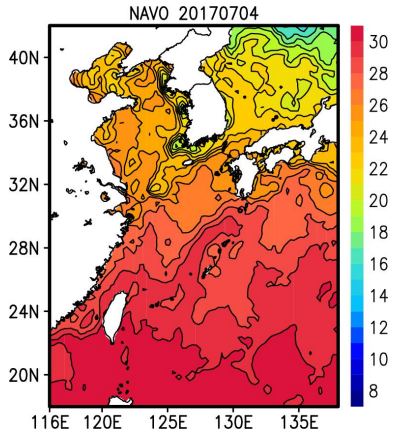

Figure 7 Horizontal distribution of daily mean NAVO SST on July 4th, 2017.

Sensitivity experiments

In order to evaluate the responses of the mesoscale convective system to the changes in the thermodynamic conditions such as SST and air-temperature, we also conduct two sensitivity experiments. The first one is referred to as AO80, in which changes in SST and vertical air-temperature profiles since 1980s are subtracted from the observed SST and the atmospheric conditions observed during the rainfall event, respectively. The second one is referred to as O80, in which only the SST change is subtracted. The air temperature in O80 is the same as that in CNTL.

Ensemble mean of area-averaged air temperature using five atmospheric datasets (NCEP1 and 2, ERA-Interim and ERA5, and JRA55) are utilized for estimating the long-term trends of air temperature (Figure 8). As in previous modeling studies, the same relative humidity (RH) field as used for CNTL was assigned as the initial and boundary conditions for the AO80, since studies of the global atmospheric moisture have found little long-term change in RH associated with the recent warming trend [Held and Soden 2006; Dai 2006; Willett et al. 2008].

Ensemble mean of area-averaged air temperature using five atmospheric datasets (NCEP1 and 2, ERA-Interim and ERA5, and JRA55) are utilized for estimating the long-term trends of air temperature (Figure 8).

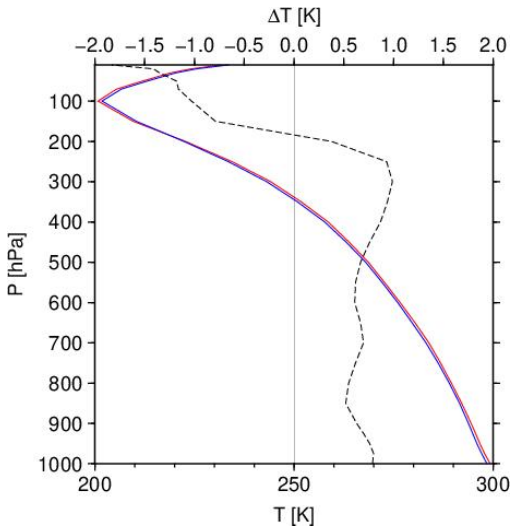

Figure 8 Vertical profiles of air temperature averaged over 22°N-42°N, 120°E-140°E in July 2017 (red) and 1980s (blue). Dashed line indicates long-term trends of air temperature in July from 1982 to 2017.

Also, ensemble mean of long-term trend is estimated using five SST datasets, namely, COBE SST, HadISST, ERSST, MGDSST, and OISST (Figure 9).

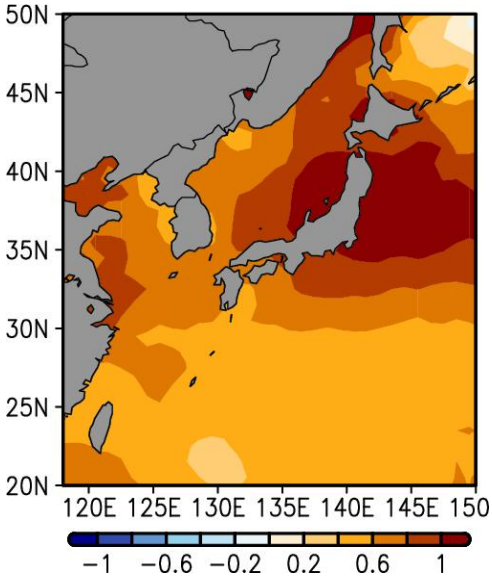

Figure 9 Ensemble mean of long-term trend of SST in July from 1982 to 2017 in K.

RESULTS

Control experiment

Figure 10 shows the horizontal distrubtion of P12 in CNTL. Overall, the model reproduces the horizontal distributions and time-change of the precipitation fairly well. Although the model does not reproduce the northern and southern weak precipitation band that appeared in the observed data, it skillfully reproduced the location and intensity of central precipitation band that exhibits . The maximum amount of the simulated P12 (~600 mm) are smaller than that of observation, but it is the same order of that in previous modelling studies [Kato 2018][Takemi 2018]. Partly because of this underestimation, the simulated P12 averaged over 33°N-34°N, 130°E-132°E (24 mm) is smaller than observed one (54 mm).

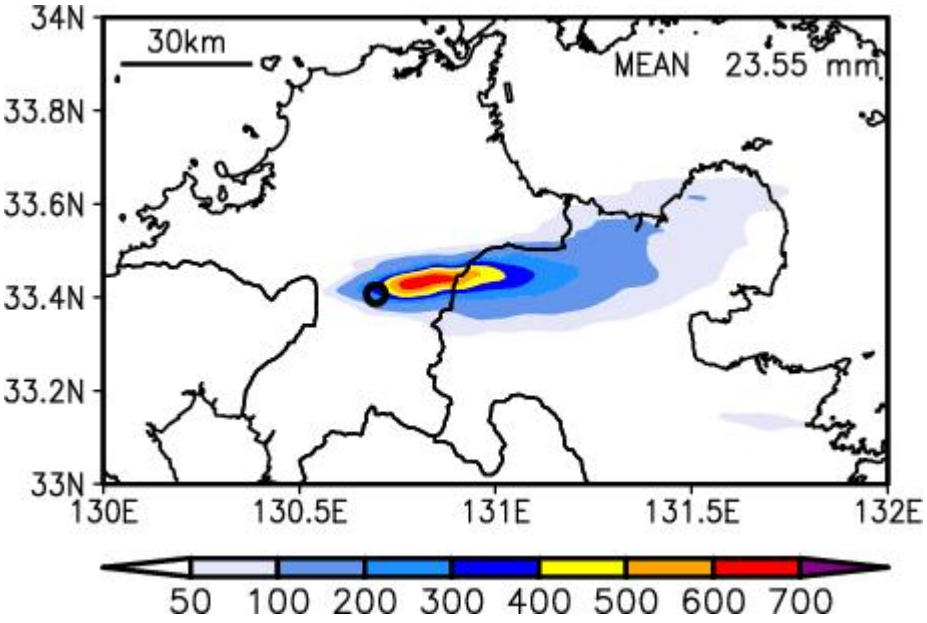

Figure 10 As in Figure 1 except for CNTL.

Time-sequence of the vertical cross-sections of simulated radar reflectivity shows consecutive development of convective clouds in the downwind direction, which is typical in the quasi-stationary convective precipitation band that cause severe flooding and landslides during warm seasons in Japan (Figure 11). The responses of this band to the SST changes are discussed in the next subsection.

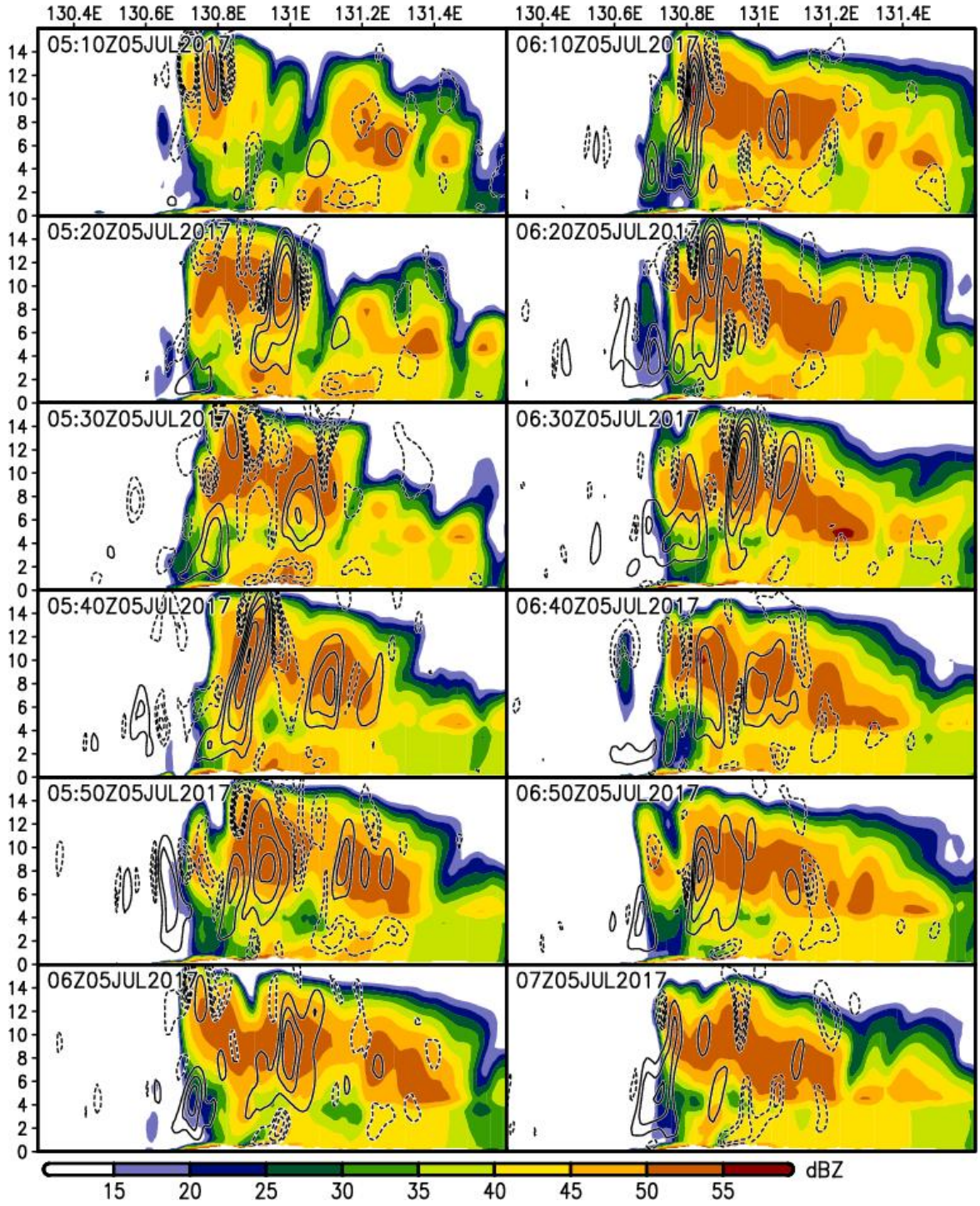

Figure 11 Time-sequence of vertical cross-section of simulated radar reflectivity (color) averaged from 33.4N to 33.5N. Abscissa is longitude and ordinate is altitude in km. Solid (dashed) contour indicate the upward (downward) vertical velocity at intervals of 5 (1) m/s.

Sensitivity experiments

The map of P12 in AO80 shows reduction of the amount of precipitation compared to CNTL (Figure 12a). The fractional change of P12 in AO80 is 6.8% with SST change of 0.64 K, which corresponds to 10.6%/K. It exceeds the value expected from the CC relationship (~6%/K) and is consistent with the estimates by a previous data analysis study (~10%/K) [Utsumi et al. 2011]. This SST change was evaluated using ensemble averages of SSTs sampled along the trajectories of 500 air parcels obtained from the backward trajectory analysis for one day starting from 00, 06, and 12 UTC 05 July 2017 in the outer domains for each experiment.

The reduction in P12 in O80 is much larger than that of AO80, highlighting the importance of SST change (Figure 12b). Atmospheric warming stabilizes the air-column and contracts the SST rise in AO80.

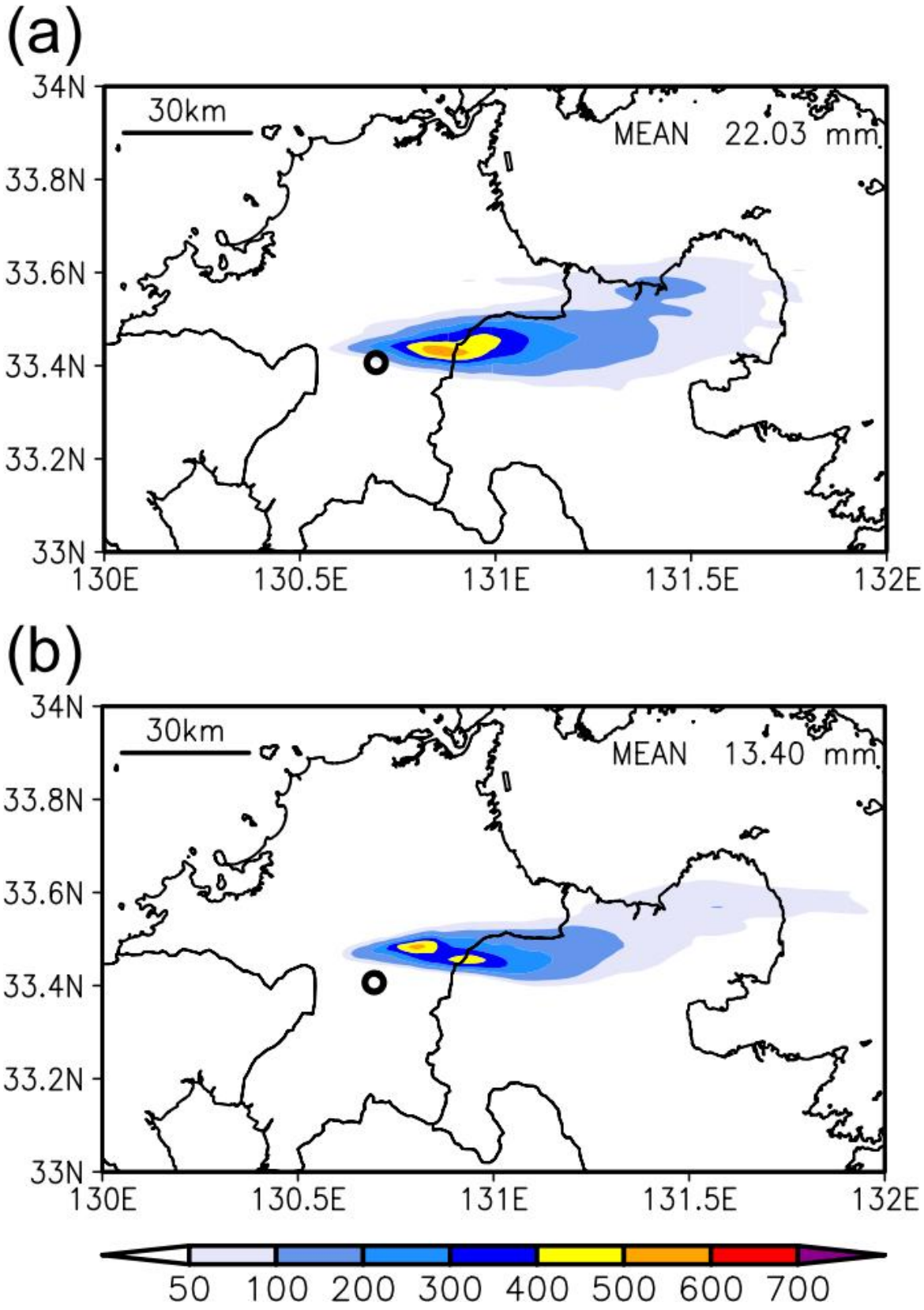

Figure 12 As in Figure 1 except for (a) AO80 and (b) O80.

The time sequence of simulated radar reflectivity and updraft velocity in AO80 clearly shows that the simulated convective systems in AO80 became weaker, compared to CNTL (Figure 13).

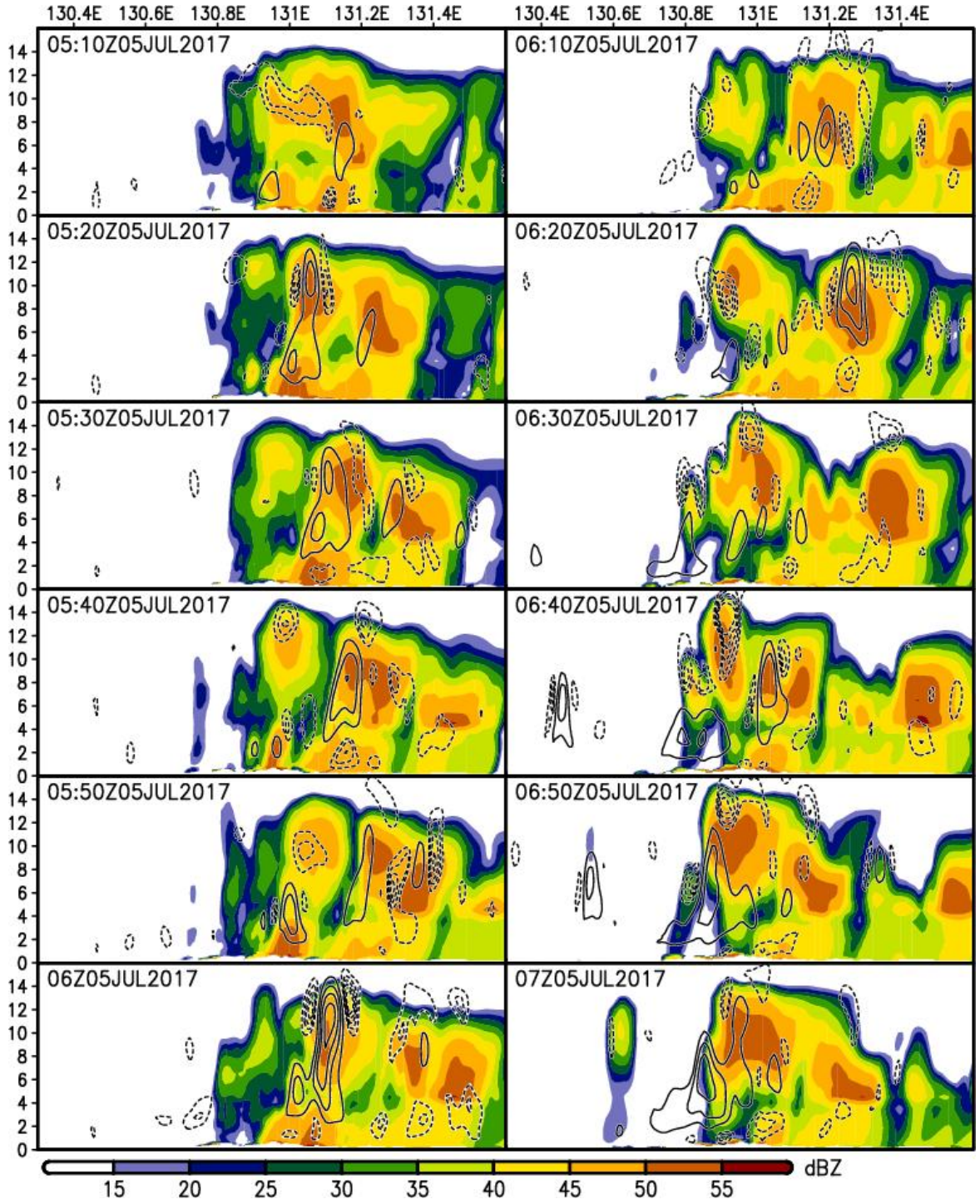

Figure 13 As in Figure 11 except for AO80.

Figure 14 shows the moisture budget in the averaged over the area where the convective systems occured based on the following equation:

$$\delta[\nabla \cdot (q\boldsymbol{v})] = \nabla \cdot (\bar{q}\delta\boldsymbol{v}) + \nabla \cdot (\bar{\boldsymbol{v}}\delta q) + \nabla \cdot (\delta\boldsymbol{v}\delta q)$$

where,

δ: difference between CNTL and AO80

q: water vapor mixing ratio

$\boldsymbol{v}$: horizontal components of wind velocity

overbar: values in CNTL

We refer to the first, second, and thrid terms in the equation above as dynamic, thermodynamic, and covariance terms, repsectively. The dynamic term dominates in changes in moisture convergence, indicating that the increase in amount of precipitation in CNTL relative to AO80 is primary due to the intentification of the convective systems and increase in precipitable water plays a secondary role.

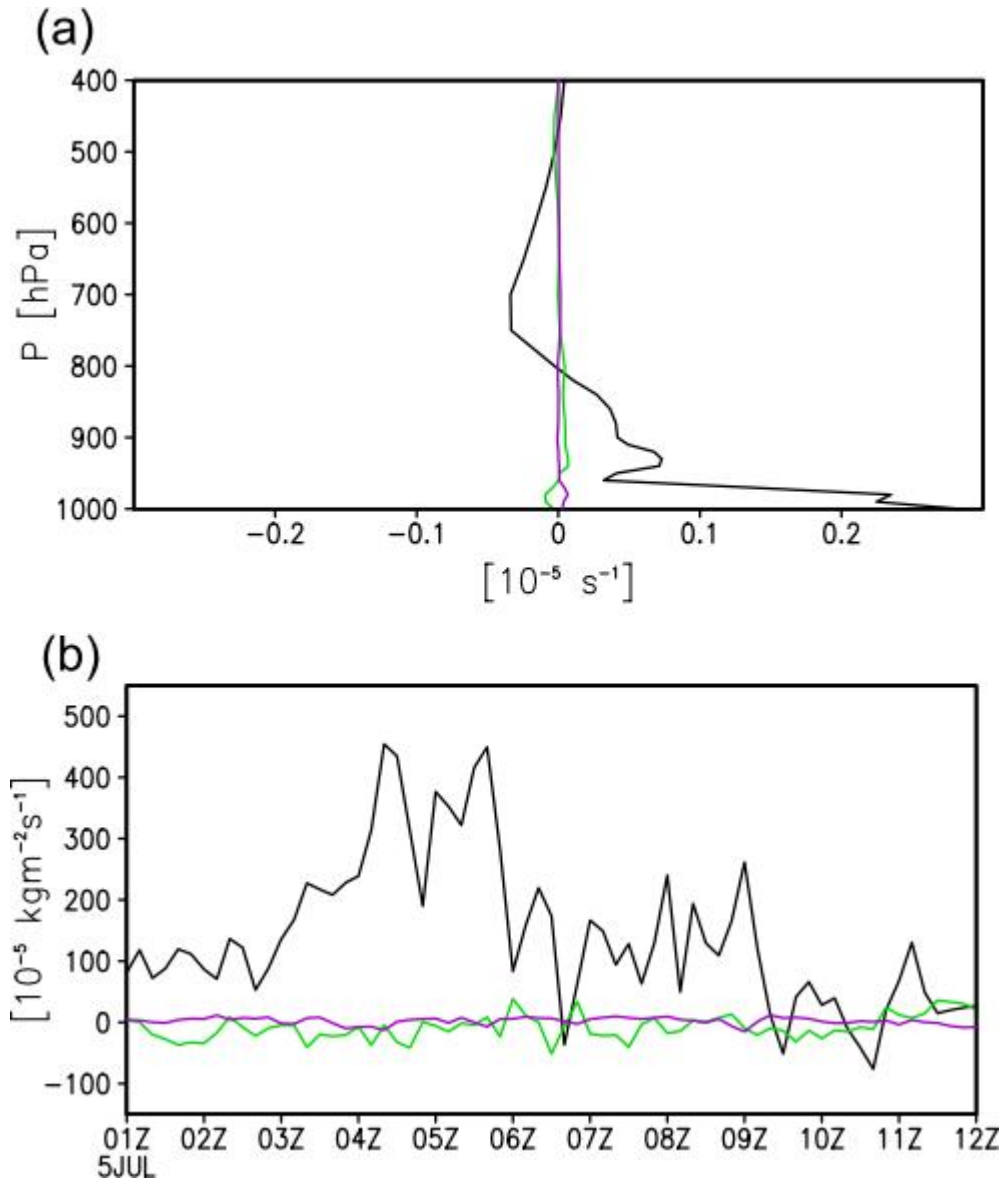

Figure 14 (a) Vertical profiles of the dynamic (black) , thermodynamic (green), and covariance (purple) terms averaged over [33.3-33.55N, 130.4-131.1E] and from 01:00 to 13:00 UTC 05JUL2017. (b) Time series of dynamic (black), thermodynamic (green), and covariance (purple) terms averaged over [33.3-33.55N, 130.4-131.1E], integrated vertically from the surface to 100 hPa pressure level.

The difference in CAPE between CNTL and AO80 clearly shows the increase in CAPE in CNTL (Figure 15). In addition, CIN exhibits slight reduction. They both provide the favorable condition for the intentification of the convective systems during this event.

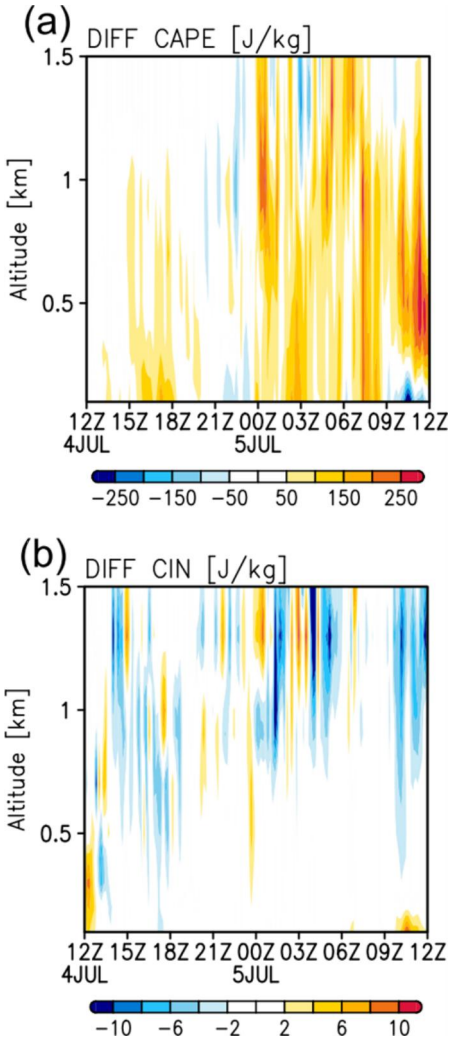

Figure 15 Time-height diagrams of differences in (a) CAPE and (b) CIN between CNTL and AO80, averaged over [33.3-33.4N, 130.5-130.6E].

CAPE is propotional to the vertical integration of the difference between EPT at the lifting condensation level (LFC) and the saturated EPT (SEPT). Figure 16 indicates the increase in CAPE in CNTL is mainly due to the increase in equivalent potential temperature near the LFC (~500m). The decrease in SEPT (i.e., tempearture) is not a primary factor in increase in CAPE. The near surface moistening in CNTL plays a primary role in increase in EPT near the LFC (Figure 16c and d). On the other hand, the contribution of the near surface warming is not large compared to that of the moistening.

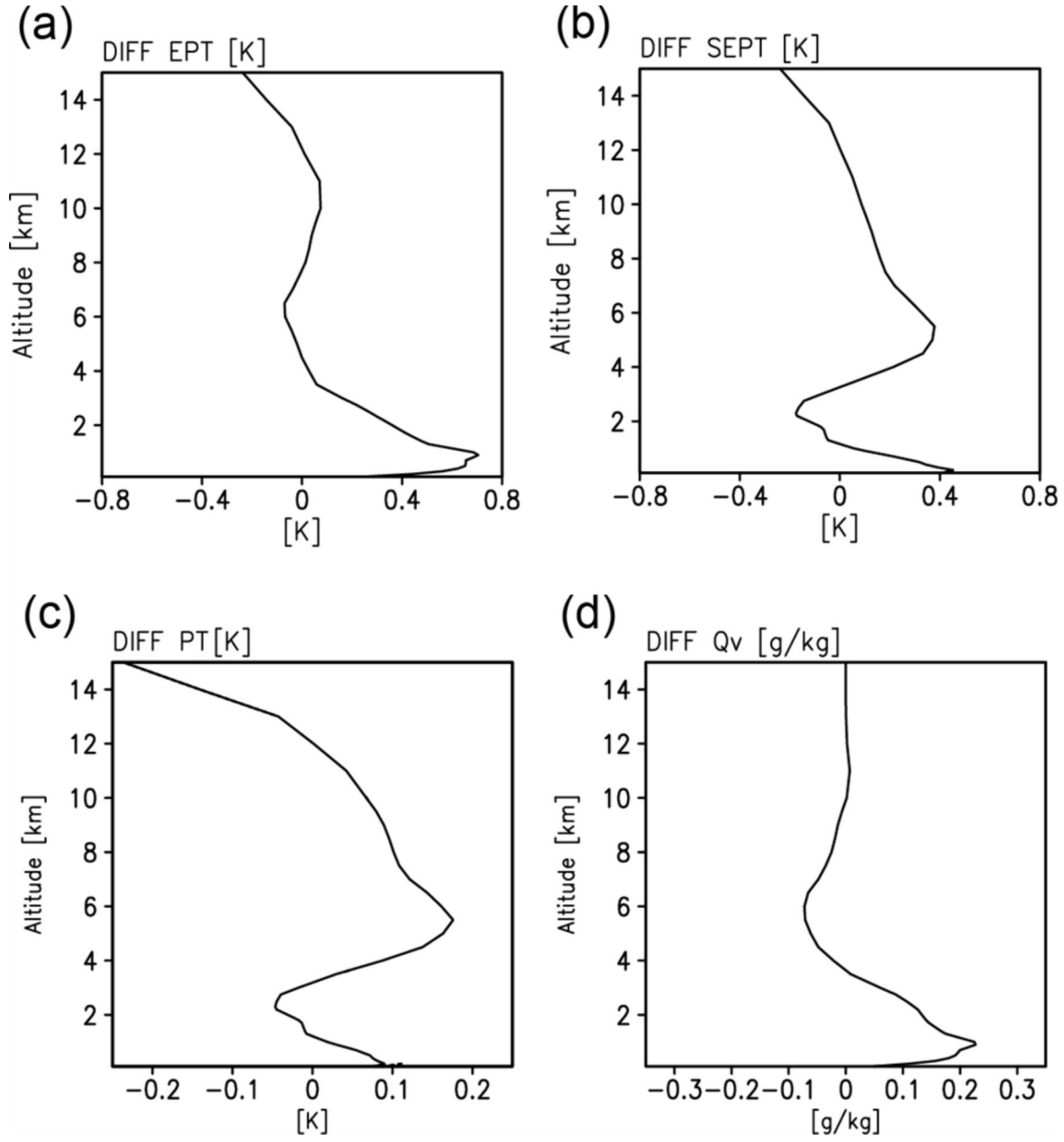

Figure 16 Vertical profiles differences in (a) EPT, (b) SEPT, (c) potential temperature, and (d) water vapor mixing ratio between CNTL and AO80, averaged over [33.3-33.4N, 130.5-130.6E], from 01 to 13 UTC 05 July, 2017.

The latent heat flux (LHF) near the Kyushu Island in CNTL is larger than that of AO80 (Figure 17).
It provides the moisture near the surface. Although the changes in moisture near the surface is rather small, it has an impact on the CAPE and hence the amount of the precipitation, suggesting the importance of the SST rise in EAMS in the intentification of the precipitation during the last three decades. In contrast, changes in the sensible heat fluix is much smaller than that in LHF.

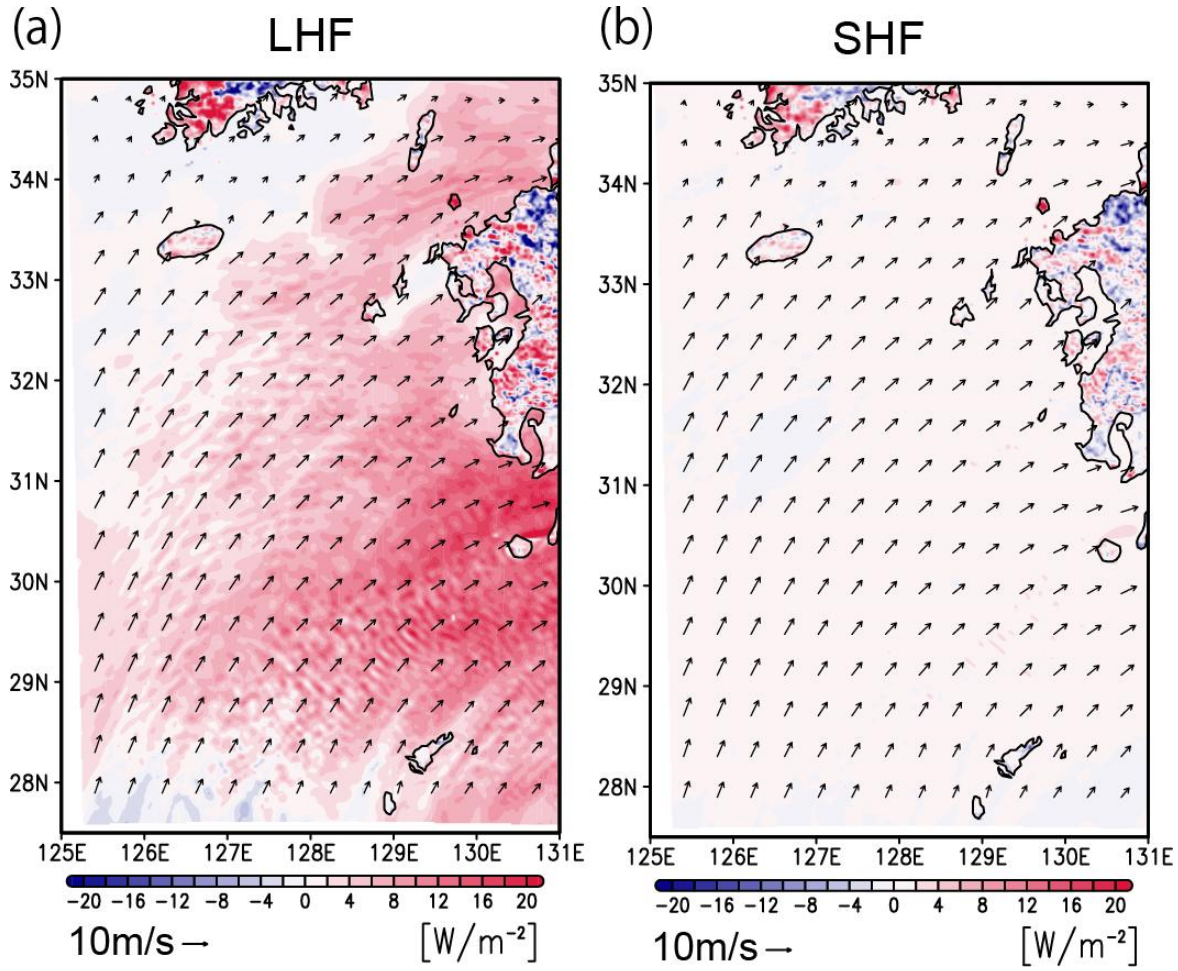

Figure 17 Horizontal distrubutions of (a) LHF and (b) SHF, averaged from 12:00 UTC 4 to 12:00 UTC 5 July, 2017.

Uncertainty due to SST datasets

Recent study indicates that the simulated rainfall is sensitive to the differences in SST among the datasets (Figure 18) [Iizuka and Nakamura 2019]. Hence, we evaluate the influence of difference in SST trends among the datasets on P12. DIfference in SST trends significantly changes P12 (Figure 19), which intruduce the uncertainty of the estimate of P12. The use of multiple SST datasets should be desirable to assess the uncertainty of P12. It also helps provide the more reliable estimate of the changes in the amount of precipitation due to the atmospheric and oceanic warming during the prast decades.

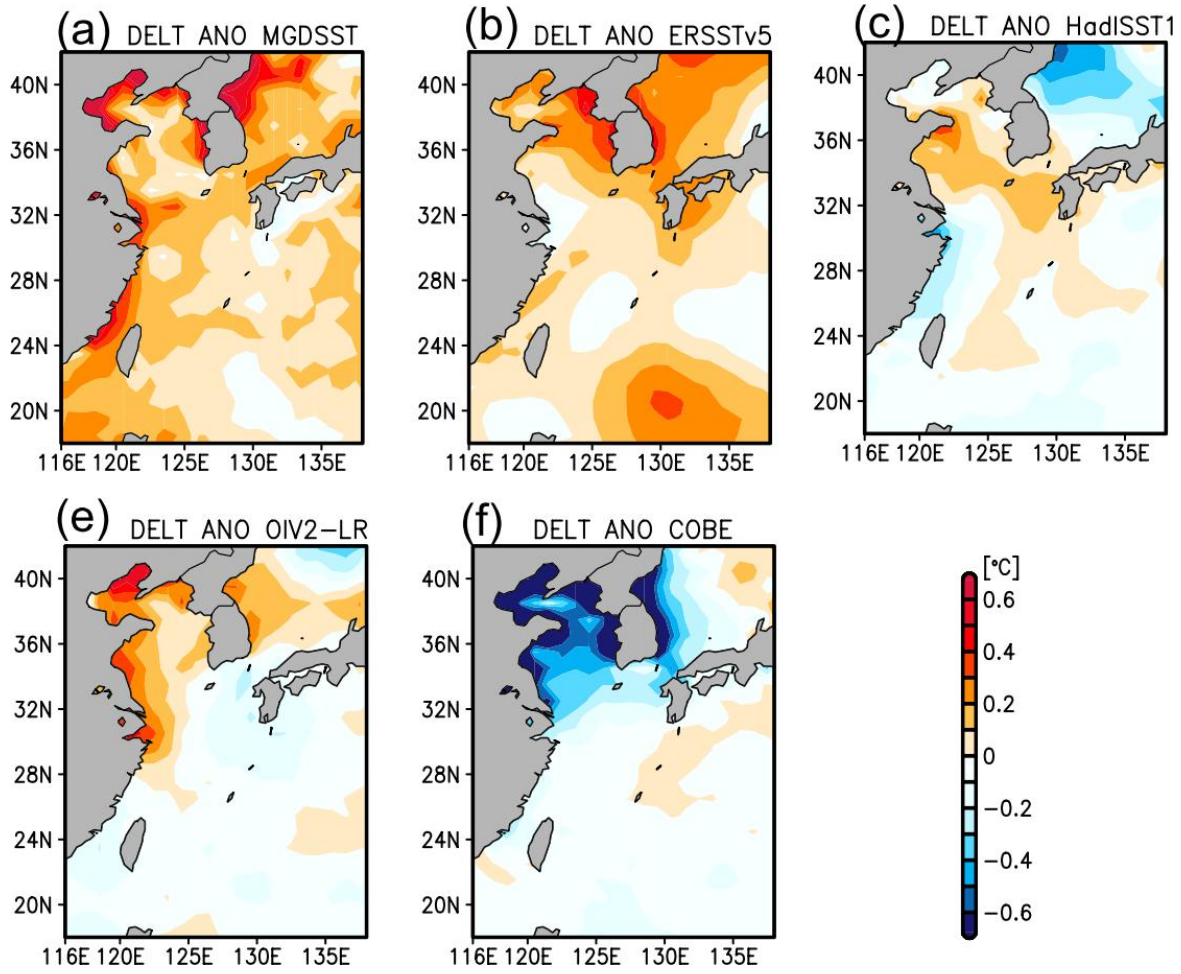

Figure 18 Horizontal distributions of anomalies of SST trends from their ensemble mean.

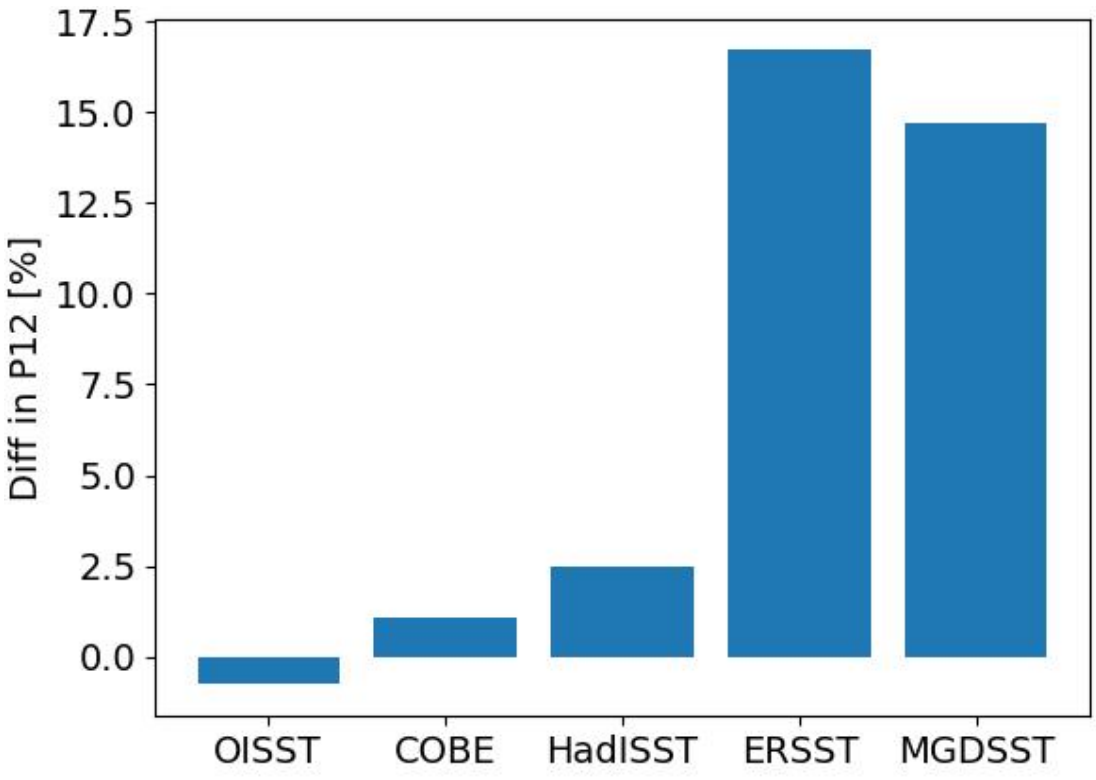

Figure 19 Fractional changes in P12 from the CNTL using the SST trends shown in Figure 18.

AUTHOR INFORMATION

Atsuyoshi Manda, PhD
Associate Professor
Mie University
1577 Kurimamachiya-cho Tsu, Mie 514-8507, JAPAN
Email: am@bio.mie-u.ac.jp

ABSTRACT

There are growing evidences that the warming marginal seas impact the torrential rainfall events in many parts of the world. The sea surface temperature (SST) in the East Asian marginal seas (EAMS) exhibits rapid rise during the last decades compared to the global mean, but its impact is still a matter of debate. Here we assess the impact of the recent warming trend of the EAMSs on the torrential rainfall event that caused devastating flooding and landslides in Kyushu Island located in the western part of Japan in July 2017, using a high-resolution cloud permitting model. The warming trend of EAMS with atmospheric warming since 1980s increases the simulated 12-hr precipitation to 6.8%, corresponding to approximately 10% increase per 1 K of SST rise, consistent with the previous data analysis study. Slight increase in heat and moisture supplies due to the warming EAMS has impacted a conditionally unstable condition of air masses flowing into an area of the precipitation, leading to more vigorous convective systems. Moisture budget analysis indicates that the changes in the amount of precipitation is not responsible for the availability of precipitable water but the intensification of the convective system. Since the change in precipitation amount exhibits high sensitivity to the SST trends, use of multiple SST datasets is desirable to provide a more reliable estimate and its uncertainty.